A CUPID Li2100MoO4scintillating bolometer tested in the CROSS underground facility

Published Version:

A CUPID Li2100MoO4scintillating bolometer tested in the CROSS underground facility / Armatol A.; Armengaud E.; Armstrong W.; Augier C.; Iii F.T.A.; Azzolini O.; Bandac I.C.; Barabash A.S.; Bari G.; Barresi A.; Baudin D.; Bellini F.; Benato G.; Beretta M.; Berge L.; Bourgeois C.; Biassoni M.; Billard J.; Boldrini V.; Branca A.; Brofferio C.; Bucci C.; Calvo-Mozota J.M.; Camilleri J.; Candela A.; Capelli S.; Cappelli L.; Cardani L.; Carniti P.; Casali N.; Cazes A.; Celi E.; Chang C.; Chapellier M.; Charrier A.; Chiesa D.; Clemenza M.; Colantoni I.; Collamati F.; Copello S.; Cremonesi O.; Creswick R.J.; Cruciani A.; D'Addabbo A.; D'Imperio G.; Dafinei I.; Danevich F.A.; De Combarieu M.; Deo M.D.; Jesus M.D.; De Marcillac P.; Dell'Oro S.; Domizio S.D.; Dompe V.; Drobizhev A.; Dumoulin L.; Fantini G.; Faverzani M.; Ferri E.; Ferri F.; Ferroni F.; Figueroa-Feliciano E.; Formaggio J.; Franceschi A.; Fu C.; Fu S.; Fujikawa B.K.; Gascon J.; Giachero A.; Gironi L.; Giuliani A.; Gorla P.; Gotti C.; Gras P.; Gros M.; Guerard E.; Gutierrez T.D.; Han K.; Hansen E.V.; Heeger K.M.; Helis D.L.; Huang H.Z.; Huang R.G.; Ianni A.; Imbert L.; Johnston J.; Juillard A.; Karapetrov G.; Keppel G.; Khalife H.; Kobychev V.V.; Kolomensky Y.G.; Konovalov S.I.; Liu Y.; Loaiza P.; Ma L.; Madhukuttan M.; Mancarella F.; Mariam R.; Marini L.; Marnieros S.; Martinez M.; Maruyama R.H.; Mauri B.; Mayer D.; Mei Y.; Milana S.; Misiak D.; Napolitano T.; Nastasi M.; Navick X.-F.; Nikkel J.; Nipoti R.; Nisi S.; Nones C.; Norman E.B.; Novosad V.; Nutini I.; O'Donnell T.; Olivier G.; Olivieri E.; Oriol C.; Ouellet J.L.; Pagan S.; Pagliarone C.; Pagnanini L.; Pari P.; Pattavina L.; Paul B.; Pavan M.; Peng H.; Pessina G.; Pettinacci V.; Pira C.; Pirro S.; Poda D.V.; Polakovic T.; Polischuk O.G.; Pozzi S.; Previtali E.; Puiu A.; Ressa A.; Reynet D.; Rizzoli R.; Rosenfeld C.; Sanglard V.; Scarpaci J.A.; Schmidt B.; Sharma V.; Shlegel V.N.; Singh V.; Sisti M.; Speller D.; Surukuchi P.T.; Taffarello L.; Tellier O.; Tomei C.; Tretyak V.I.; Tsymbaliuk A.; Velazquez M.; Vetter K.J.; Wagaarachchi S.L.; Wang G.; Wang L.; Welliver B.; Wilson J.; Wilson K.; Winslow L.A.; Xue M.; Yan L.; Yang J.; Yefremenko V.; Yumatov V.I.; Zarytskyy M.M.; Zhang J.; Zolotarova A.S.; Zucchelli S.. - In: JOURNAL OF INSTRUMENTATION. - ISSN 1748-0221. - STAMPA. - 16:2(2021), pp. P02037.1-P02037.16. [10.1088/1748-0221/16/02/P02037]

Availability:
This version is available at: https://hdl.handle.net/11585/843639 since: 2022-01-15

Published:
DOI: http://doi.org/10.1088/1748-0221/16/02/P02037

20 April 2024

A. Armatol et al, *A CUPID Li2100MoO4 scintillating bolometer tested in the CROSS underground facility*, 2021 JINST 16 P02037.

The final published version is available online at: https://doi.org/10.1088/1748-0221/16/02/P02037

Prepared for submission to JINST

A CUPID $Li_2{}^{100}MoO_4$ scintillating bolometer tested in the CROSS underground facility

---

A. Armatol,[a] E. Armengaud,[a] W. Armstrong,[b] C. Augier,[c] F. T. Avignone III,[d] O. Azzolini,[e] I. C. Bandac,[f] A. S. Barabash,[g] G. Bari,[h] A. Barresi,[i,j] D. Baudin,[a] F. Bellini,[k,l] G. Benato,[m] M. Beretta,[n] L. Bergé,[o] Ch. Bourgeois,[o] M. Biassoni,[i] J. Billard,[c] V. Boldrini,[p,h] A. Branca,[i,j] C. Brofferio,[i,j] C. Bucci,[m] J. M. Calvo-Mozota,[f] J. Camilleri,[q] A. Candela,[m] S. Capelli,[i,j] L. Cappelli,[m] L. Cardani,[k] P. Carniti,[i,j] N. Casali,[k] A. Cazes,[c] E. Celi,[m,r] C. Chang,[b] M. Chapellier,[o] A. Charrier,[s] D. Chiesa,[i,j] M. Clemenza,[i,j] I. Colantoni,[k,t] F. Collamati,[k] S. Copello,[u,v] O. Cremonesi,[i] R. J. Creswick,[d] A. Cruciani,[k] A. D'Addabbo,[m,r] G. D'Imperio,[k] I. Dafinei,[k] F. A. Danevich,[w] M. de Combarieu,[s] M. De Deo,[m] M. De Jesus,[c] P. de Marcillac,[o] S. Dell'Oro,[i,j] S. Di Domizio,[u,v] V. Dompe,[m,r] A. Drobizhev,[x] L. Dumoulin,[o] G. Fantini,[k,l] M. Faverzani,[i,j] E. Ferri,[i,j] F. Ferri,[a] F. Ferroni,[k,r] E. Figueroa-Feliciano,[y] J. Formaggio,[z] A. Franceschi,[aa] C. Fu,[ab] S. Fu,[ab] B. K. Fujikawa,[x] J. Gascon,[c] A. Giachero,[i,j] L. Gironi,[i,j] A. Giuliani,[o] P. Gorla,[m] C. Gotti,[i] P. Gras,[a] M. Gros,[a] E. Guerard,[o] T. D. Gutierrez,[ac] K. Han,[ad] E. V. Hansen,[n] K. M. Heeger,[ae] D. L. Helis,[a] H. Z. Huang,[ab,af] R. G. Huang,[n,x] A. Ianni,[m] L. Imbert,[o] J. Johnston,[z] A. Juillard,[c] G. Karapetrov,[ag] G. Keppel,[e] H. Khalife,[o] V. V. Kobychev,[w] Yu. G. Kolomensky,[n,x] S. I. Konovalov,[g] Y. Liu,[ah] P. Loaiza,[o] L. Ma,[ab] M. Madhukuttan,[o] F. Mancarella,[p,h] R. Mariam,[o] L. Marini,[n,x,m] S. Marnieros,[o] M. Martinez,[ai,aj] R. H. Maruyama,[ae] B. Mauri,[a] D. Mayer,[z] Y. Mei,[x] S. Milana,[k] D. Misiak,[c] T. Napolitano,[aa] M. Nastasi,[i,j] X.-F. Navick,[a] J. Nikkel,[ae] R. Nipoti,[p,h] S. Nisi,[m] C. Nones,[a] E. B. Norman,[n,ak] V. Novosad,[b] I. Nutini,[i,j] T. O'Donnell,[q] G. Olivier,[o] E. Olivieri,[o] C. Oriol,[o] J. L. Ouellet,[z] S. Pagan,[ae] C. Pagliarone,[m] L. Pagnanini,[m,r] P. Pari,[s] L. Pattavina,[m,1] B. Paul,[a] M. Pavan,[i,j] H. Peng,[al] G. Pessina,[i] V. Pettinacci,[k] C. Pira,[e] S. Pirro,[m] D. V. Poda,[o] T. Polakovic,[b] O. G. Polischuk,[w] S. Pozzi,[i,j] E. Previtali,[i,j] A. Puiu,[m,r] A. Ressa,[k,l] D. Reynet,[o] R. Rizzoli,[p,h] C. Rosenfeld,[d] V. Sanglard,[c] J. A. Scarpaci,[o] B. Schmidt,[y,x] V. Sharma,[q] V. N. Shlegel,[am] V. Singh,[n] M. Sisti,[i] D. Speller,[an,ae] P. T. Surukuchi,[ae] L. Taffarello,[ao] O. Tellier,[a] C. Tomei,[k] V. I. Tretyak,[w] A. Tsymbaliuk,[e] M. Velazquez,[ap] K. J. Vetter,[n] S. L. Wagaarachchi,[n] G. Wang,[b] L. Wang,[ah] B. Welliver,[x] J. Wilson,[d] K. Wilson,[d] L. A. Winslow,[z] M. Xue,[al] L. Yan,[ab] J. Yang,[al] V. Yefremenko,[b] V. I. Yumatov,[g] M. M. Zarytskyy,[w] J. Zhang,[b] A. S. Zolotarova,[o] S. Zucchelli[h,aq]

[a] *IRFU, CEA, Université Paris-Saclay, F-91191 Gif-sur-Yvette, France*
[b] *Argonne National Laboratory, Argonne, IL 60439, USA*
[c] *Univ Lyon, Université Lyon 1, CNRS/IN2P3, IP2I-Lyon, F-69622, Villeurbanne, France*
[d] *Department of Physics and Astronomy, University of South Carolina, Columbia, SC 29208, USA*

---

[1] Also at: Physik-Department, Technische Universität München, Garching, Germany

[e]*INFN – Laboratori Nazionali di Legnaro, Legnaro (Padova) I-35020, Italy*
[f]*Laboratorio Subterráneo de Canfranc, 22880 Canfranc-Estación, Spain*
[g]*National Research Centre Kurchatov Institute, Institute of Theoretical and Experimental Physics, 117218 Moscow, Russia*
[h]*INFN – Sezione di Bologna, Bologna I-40127, Italy*
[i]*INFN – Sezione di Milano Bicocca, Milano I-20126, Italy*
[j]*Dipartimento di Fisica, Università di Milano-Bicocca, Milano I-20126, Italy*
[k]*INFN – Sezione di Roma, Roma I-00185, Italy*
[l]*Dipartimento di Fisica, Sapienza Università di Roma, Roma I-00185, Italy*
[m]*INFN – Laboratori Nazionali del Gran Sasso, I-67100 Assergi (AQ), Italy*
[n]*University of California, Berkeley, CA 94720, USA*
[o]*Université Paris-Saclay, CNRS/IN2P3, IJCLab, 91405 Orsay, France*
[p]*Istituto per la Microelettronica e Microsistemi, Consiglio Nazionale delle Ricerche, 40129, Bologna, Italy*
[q]*Center for Neutrino Physics, Virginia Polytechnic Institute and State University, Blacksburg, Virginia 24061, USA*
[r]*INFN – Gran Sasso Science Institute, L'Aquila I-67100, Italy*
[s]*IRAMIS, CEA, Université Paris-Saclay, F-91191 Gif-sur-Yvette, France*
[t]*Istituto di Nanotecnologia, Consiglio Nazionale delle Ricerche, c/o Dip. Fisica, Sapienza Università di Roma, 00185 Roma, Italy*
[u]*INFN – Sezione di Genova, Genova I-16146, Italy*
[v]*Dipartimento di Fisica, Università di Genova, Genova I-16146, Italy*
[w]*Institute for Nuclear Research of NASU, 03028 Kyiv, Ukraine*
[x]*Lawrence Berkeley National Laboratory, Berkeley, CA 94720, USA*
[y]*Department of Physics & Astronomy, Northwestern University, Evanston, IL 60208-3112, USA*
[z]*Massachusetts Institute of Technology, Cambridge, MA 02139, USA*
[aa]*INFN – Laboratori Nazionali di Frascati, Frascati (Roma) I-00044, Italy*
[ab]*Key Laboratory of Nuclear Physics and Ion-beam Application (MOE), Fudan University, Shanghai 200433, China*
[ac]*Physics Department, California Polytechnic State University, San Luis Obispo, CA 93407, USA*
[ad]*INPAC and School of Physics and Astronomy, Shanghai Jiao Tong University; Shanghai Laboratory for Particle Physics and Cosmology, Shanghai 200240, China*
[ae]*Wright Laboratory, Department of Physics, Yale University, New Haven, CT 06520, USA*
[af]*Department of Physics and Astronomy, University of California, Los Angeles, CA 90095, USA*
[ag]*Department of Physics, Drexel University, Philadelphia, PA 19104, USA*
[ah]*Beijing Normal University, Beijing 100875, China*
[ai]*Laboratorio de Fisica Nuclear y Astroparticulas, Universidad de Zaragoza, 50009 Zaragoza, Spain*
[aj]*aj Fundación Agencia Aragonesa para la Investigación y el Desarrollo, 50018 Zaragoza, Spain*
[ak]*Lawrence Livermore National Laboratory, Livermore, CA 94550, USA*
[al]*Department of Modern Physics, University of Science and Technology of China, Hefei 230027, China*
[am]*Nikolaev Institute of Inorganic Chemistry, 630090 Novosibirsk, Russia*
[an]*Johns Hopkins University, Baltimore, MD 21218, USA*
[ao]*INFN – Sezione di Padova, Padova I-35131, Italy*
[ap]*Université Grenoble Alpes, CNRS, Grenoble INP, SIMAP, 38402 Saint Martin d'Héres, France*
[aq]*Dipartimento di Fisica e Astronomia, Alma Mater Studiorum – Università di Bologna, Bologna I-40127, Italy*

E-mail: `cupid.publications@lngs.infn.it`, `cross.publications@lsc-canfranc.es`

Abstract: A scintillating bolometer based on a large cubic $Li_2{}^{100}MoO_4$ crystal (45 mm side) and a Ge wafer (scintillation detector) has been operated in the CROSS cryogenic facility at the Canfranc underground laboratory in Spain. The dual-readout detector is a prototype of the technology that will be used in the next-generation $0\nu2\beta$ experiment CUPID. The measurements were performed at 18 and 12 mK temperature in a pulse tube dilution refrigerator. This setup utilizes the same technology as the CUORE cryostat that will host CUPID and so represents an accurate estimation of the expected performance. The $Li_2{}^{100}MoO_4$ bolometer shows a high energy resolution of 6 keV FWHM at the 2615 keV γ line. The detection of scintillation light for each event triggered by the $Li_2{}^{100}MoO_4$ bolometer allowed for a full separation ($\sim 8\sigma$) between $\gamma(\beta)$ and α events above 2 MeV. The $Li_2{}^{100}MoO_4$ crystal also shows a high internal radiopurity with ^{228}Th and ^{226}Ra activities of less than 3 and 8 μBq/kg, respectively. Taking also into account the advantage of a more compact and massive detector array, which can be made of cubic-shaped crystals (compared to the cylindrical ones), this test demonstrates the great potential of cubic $Li_2{}^{100}MoO_4$ scintillating bolometers for high-sensitivity searches for the ^{100}Mo $0\nu2\beta$ decay in CROSS and CUPID projects.

Keywords: Double-beta decay, Cryogenic detector, Bolometer, Crystal scintillator, Lithium molybdate, Particle identification, Radiopurity

ArXiv ePrint: 2011.13806

Contents

1 Introduction

Neutrinoless double-beta ($0\nu2\beta$) decay is a unique probe of new physics beyond the Standard Model [**? ?**] and the observation of this process, suggested about 80 years ago but not yet detected (in contrast to two-neutrino double-beta ($2\nu2\beta$) decay [**?**]), would conclusively demonstrate lepton number violation and the Majorana nature of neutrinos (i.e. a particle that is equal to its own anti-particle).

The bolometric technology, which relies on the use of low-temperature calorimeters acting simultaneously as a 2β source and a detector, is among the few experimental approaches providing world-leading sensitivity to $0\nu2\beta$ decay to-date [**?**]. In addition to high detection efficiency of the "2β source = detector" technique, bolometers offer high energy resolution, scalability to a large detector mass via arrays of modules, and the possibility to use different and radiopure materials containing the most promising 2β isotopes (e.g. see [**? ? ?**]). Additionally, recent technological advances have demonstrated the ability to do particle identification [**? ? ?**], allowing for a reduction of backgrounds in the signal region of interest by multiple orders of magnitude.

Bolometric techniques for $0\nu2\beta$ decay searches have been developed for about 30 years and have resulted in the first tonne-scale bolometric experiment CUORE (Cryogenic Underground Observatory of Rare Events) [**?**]. CUORE has been in operation at the Gran Sasso underground laboratory (Italy) since 2017, searching for $0\nu2\beta$ decay of ^{130}Te (Q-value of the 2β transition, $Q_{2\beta}$, is 2528 keV [**?**]). In spite of this extraordinary achievement, the CUORE $0\nu2\beta$ sensitivity is limited by a background ($\sim10^{-2}$ counts/yr/kg/keV) coming from alpha decays at surfaces despite the highly radiopure materials used for the detector construction. This is due to the use of pure thermal detectors based on tellurium dioxide crystals (TeO_2; 34% of ^{130}Te in natural tellurium [**?**]) which have the same bolometric response irrespective of the type of the particle interaction [**?**].

CUPID (CUORE Upgrade with Particle IDentification) is a proposed next-generation $0\nu2\beta$ bolometric experiment [?], which will reuse the CUORE infrastructure for the operation of a similar-scale isotopically enriched detector with a background $\sim10^{-4}$ counts/yr/kg/keV in the region of interest, thus probing $0\nu2\beta$ decay in so-called "zero-background" conditions. The suppression of the alpha-induced background to a negligible level (i.e. 99.9% of alpha events rejection), while keeping almost 100% of the signal efficiency, is required for particle identification technology. The detector performance is expected to be similar to CUORE and predecessors, with a 5 keV FWHM at $Q_{2\beta}$ as a goal. The activities of ^{226}Ra, ^{228}Th, and ^{232}Th in the enriched bolometers are required to be less than 10 μBq/kg, making the contribution of the U/Th crystal bulk activity to be below $\sim10^{-4}$ counts/yr/kg/keV. The total bulk radioactivity of the crystals should not exceed the mBq/kg level to avoid impacting the detector operation and background with pile-ups [? ? ? ?].

Four isotopes, ^{82}Se ($Q_{2\beta}$ = 2998 keV [?]), ^{100}Mo (3034 keV [?]), ^{116}Cd (2813 keV [?]) and ^{130}Te, were considered in the CUPID R&D program [?] as isotopes of interest to be embedded in the CUPID detector for the following reasons:

- The $0\nu2\beta$ decay energy of these isotopes (except for ^{130}Te) is greater than 2.6 MeV, the end-point of the most energetic intense natural γ-ray radiation;
- Enrichment is available at a large amount and reasonable cost;
- Compounds containing these isotopes can be grown into single crystals usable for cryogenic applications;
- Some of Se-, Mo-, or Cd-containing crystals are also reasonably efficient low-temperature scintillators. The detection of scintillation light using an auxiliary optical bolometer in coincidences with the measurement of particle-induced energy release in the scintillating absorber is a viable tool for particle identification. This technique can also be applied for poorly or non-scintillating crystals, as TeO_2, to detect Cherenkov radiation allowing particle identification (however, more performing light detectors are demanded to detect a tiny signal).

Efficient alpha background rejection has been demonstrated with detectors containing each of these isotopes [? ? ? ? ?]. This paves the way for a future study of $0\nu2\beta$ across multiple isotopes [?] in case a discovery is made. Based on performance and cost, CUPID selected ^{100}Mo embedded in lithium molybdate (Li_2MoO_4) scintillating crystals [?].

The technology of ^{100}Mo-enriched lithium molybdate ($Li_2{}^{100}MoO_4$) scintillating bolometers has been recently developed within the LUMINEU project and it provides [? ?]:

- A know-how for the mass production of high-quality large radiopure crystals with only few % losses of the enriched material;
- The fabrication of a detector module (which can be easily mount into array) with energy resolution comparable to that of TeO_2 bolometers, but with a significantly higher α rejection efficiency (e.g. see in [?]).

Excellent performances of $Li_2{}^{100}MoO_4$ scintillating bolometers based on cylindrical crystals (⌀44×45 mm, ~0.21 kg, ~97% enrichment in ^{100}Mo) have been demonstrated in single-module and 4-crystal-array tests of LUMINEU [? ? ?] at the Gran Sasso and Modane (LSM; France) underground laboratories. These results have been recently confirmed by the CUPID-Mo experiment [? ? ?] on the scale of a 20-detector array operated at the LSM. Furthermore, the crystal production protocol, adopted by LUMINEU and CUPID-Mo, has been used for the fabrication of 32 $Li_2{}^{100}MoO_4$ crystals 0.28 kg each (the average enrichment in ^{100}Mo is 97.7(3)%) for the CROSS (Cryogenic Rare-event Observatory with Surface Sensitivity) $0\nu2\beta$ experiment [?].

CROSS, considered as a part of CUPID R&D, is a project aiming at the development of $Li_2{}^{100}MoO_4$ and $^{130}TeO_2$ surface-coated bolometers capable of identifying a near surface particle interaction via pulse-shape analysis [?]. A key ingredient of the CROSS technology is crystal-surface coating with a superconducting material to modify the signal pulse-shape for an event occurring at its proximity. The CROSS detector performance and radiopurity should be in compliance with CUPID requirements. The feasibility of a highly-efficient identification of near-surface α interactions has recently been demonstrated in multiple tests of the CROSS prototypes [? ? ? ?]. A final validation of the technology is planned to be realized as a $0\nu2\beta$ experiment with at least 32 $Li_2{}^{100}MoO_4$ bolometers (the addition of the 20 crystals from CUPID-Mo are now also in consideration), hosted in a dedicated cryostat at the Canfranc underground laboratory (Spain). The sensitivity of this medium-scale demonstrator [?] is expected to be on the level of the leading $0\nu2\beta$ experiments, which have masses larger by a factor 10–100.

In contrast to LUMINEU and CUPID-Mo, CROSS is going to use cubic $Li_2{}^{100}MoO_4$ elements with a 45 mm side. The choice of a cubic shape is driven by the possibility to realize a more compact array structure, which allows to deploy a ∼ 30% higher isotope mass in the available experimental volume, and yields an enhanced efficiency in rejecting background-like events that release energy in neighboring crystals (coincidences). Indeed, a volume (i.e. mass) of a cylindrical crystal with a diameter and height equal to the side of the cubic one is almost 30% less (similar to CUPID-Mo vs. CROSS crystals). It is also evident that the efficiency of coincidences between larger, particularly neighbor, detectors would be increased too. The CROSS development of an array of cubic $Li_2{}^{100}MoO_4$ bolometers is also an important benchmark for the design of the final CUPID structure, initially considered to be based on cylindrical ($\oslash 50 \times 50$ mm) $Li_2{}^{100}MoO_4$ scintillating bolometers [?]. Before using the crystals in the CROSS and CUPID $0\nu2\beta$ experiments, it is necessary to perform low-temperature test(s) to demonstrate that:

- Bolometric and spectrometric performances of cubic-shaped $Li_2{}^{100}MoO_4$ scintillating bolometers, operated in modern pulse-tube cryostats with possible vibration disturbances, are similar to those of cylindrical $Li_2{}^{100}MoO_4$ detectors tested in dry and/or wet dilution refrigerators;

- Scintillation light yield of the cubic-shaped and cylindrical crystals is similar, thus providing a highly efficient particle identification;

- Radioactive contamination of cubic $Li_2{}^{100}MoO_4$ crystals is compatible to that of cylindrical ones.

With these goals in mind, we realized a first investigation of a scintillating bolometer based on a large-volume (∼90 cm^3) cubic-shaped $Li_2{}^{100}MoO_4$ crystal, described in the present paper. This study is undertaken as part of both the CROSS and CUPID R&D programs.

2 Detector construction and operation

2.1 $Li_2{}^{100}MoO_4$ scintillating bolometer fabrication

We construct a dual-readout cryogenic particle detector from a primary scintillating absorber and a light detector. The $Li_2{}^{100}MoO_4$ absorber consists of a 45×45×45 mm crystal (~98% enrichment in ^{100}Mo) of mass 279.42 g. We randomly chose the sample from the batch of 32 identical crystals. The crystals were grown starting from purified ^{100}Mo powder and using the low-temperature-gradient technique at the Nikolaev Institute of Inorganic Chemistry (Novosibirsk, Russia). The $Li_2{}^{100}MoO_4$ samples are not perfectly cubic-shaped[1] due to not optimal growing conditions (in particular, the platinum crucible size was not large enough), adapted for the growth of up to ⌀50 mm crystal boules [? ? ?]. A Neutron Transmutation Doped (NTD) Ge thermistor [?] with a size of 3×3×1 mm and a P-doped Si chip [?] were epoxy-glued on the crystal top. The dependency of the NTD Ge resistance on temperature can be approximated as $R(T) = R_0 \cdot e^{(T_0/T)^{0.5}}$ with the parameters $T_0 \sim 3.8$ K and $R_0 \sim 1.5\ \Omega$. The Si chip is used as a resistive element to periodically inject constant energy pulses used for off-line stabilization of the bolometric response [?]. The crystal holder is made from copper to host cubic crystals of up to 5 cm side and optical bolometers at their top and/or bottom [? ? ?]. As for the light detector (LD) we use a SiO-coated Ge wafer of 44 mm diameter and 0.175 mm thickness, instrumented with a 3×1×1 mm NTD. The LD was mounted in the copper holder near the $Li_2{}^{100}MoO_4$ detector (LMO).

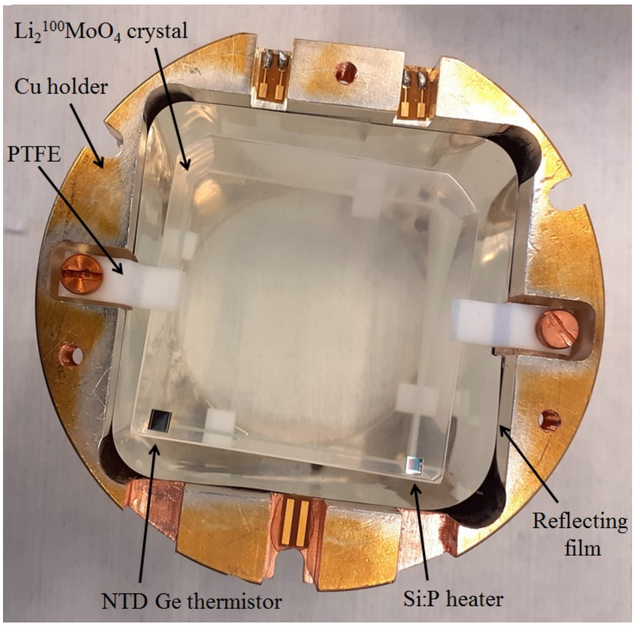

Figure 1. A photograph of the partially assembled $Li_2{}^{100}MoO_4$ scintillating bolometer; the construction elements (see text) are labeled. A ⌀45 mm hole at the bottom of the holder, visible in transparency, acts as an entrance window for the $Li_2{}^{100}MoO_4$ scintillation light to be registered by a bolometric Ge light detector.

The crystal is fixed inside the copper holder by PTFE (polytetrafluoroethylene) pieces, as seen in Fig. 1. The PTFE supports act also as thermal contacts to the heat sink of the cryostat.

---

[1] There are edge chamfers on the crystals, see Fig. 1.

The Cu holder of the detector is coated with Au to avoid oxidation, while the internal part of the holder is also coated with Ag to improve light reflection. The $Li_2{}^{100}MoO_4$ crystal inside the Cu housing is surrounded with a Vikuiti™ reflecting film, which is the same used in LUMINEU and CUPID-Mo. The NTD Ge is wire-bonded with Au wires, while the heater is bonded with Al wires. A $^{238}U/^{234}U$ source is placed on the holder's top cap. The source was obtained by depositing an uranium-containing liquid drop on a thin copper substrate that was then dried by evaporation. Part of the alpha particles (as well as nuclear recoils) emitted are degraded in energy. The LD is fabricated in the same way using a dedicated Cu holder, three PTFE elements, and an NTD Ge sensor glued. A ^{55}Fe X-ray source is placed close to the LD to irradiate the Ge surface opposite to the $Li_2{}^{100}MoO_4$ absorber.

2.2 Low-temperature underground measurements

We tested the detector in the CROSS Cryogenic Underground (C2U) facility [**?**], in operation at the Canfranc laboratory (Spain) since April 2019. The cryostat is placed inside a Faraday cage with acoustic isolation, formerly used by the ROSEBUD dark matter experiment [**?**]. The set-up operates a pulse-tube (Cryomech PT415) based dilution refrigerator, developed by CryoConcept (France), which is also assisted by Ultra Quiet Technology™ (UQT) to mitigate vibrations [**?**]. During the cryostat commissioning, it was found the UQT to efficiently reduce vibrations in the vertical direction, but not as much horizontally [**?**] resulting in a noise excess affecting the bolometric performance [**?**]. Thus, the hybrid bolometer was spring-suspended from the detector plate. In order to reduce the environmental background, the cryostat is surrounded externally by a 25 cm thick low-radioactivity lead shield. Moreover, the detector volume inside the cryostat is shielded from the dilution unit and cryostat upper parts with a 13 cm thick disk made of sandwiched lead and copper (120 kg total mass). The shielding of the set-up has not been completed yet, in particular an anti-radon Plexiglas box (to be flushed with a deradonized air) and a muon veto will be installed soon.

The signal readout is based on a low-noise room-temperature DC front-end electronics [**?**] tracing back to the Cuoricino experiment. The data acquisition (DAQ) is a new design candidate for CUPID [**?**] and consists of two 12-channel boards with a programmable 6-pole Bessel-Thomson anti-aliasing filter and integrated 24-bit ADC. A cut-off frequency of the low-pass filter can be set from 24 Hz up to 2.5 kHz. With the 24 bit ADC resolution, the input noise is not limited by the ADC even with the lowest gain value set at a programmable-gain amplifier (PGA). An additional advantage of such ADC resolution is that the PGA stage can be made much simpler or removed, with less power consumption, cost, and space. The sampling rate up to 25 kS/s can be set (250 kS/s with half of channels). The ADC-digitized continuous data are readout by an external FPGA (field-programmable gate array) module and then transferred to a personal computer via Ethernet. The DAQ control is done with the help of a MATLAB-based graphical user interface program. The monitoring on-line of the data quality is realized as a LabVIEW application.

We collected data from the end of December 2019 until the beginning of April 2020. The measurements were performed at temperatures 18 and 12 mK. We periodically calibrated the LMO by inserting a thoriated tungsten wire inside the lead shield. We chose the working points for both operational temperatures to be a few nA current on the NTD sensor resulting in a few MΩ resistance. The data are sampled continuously at a 2 kS/s sampling rate, and the full data stream is

Table 1. Performance of a scintillating bolometer based on the $\oslash$44 mm Ge light detector coupled to the 45 mm side $Li_2{}^{100}MoO_4$ cubic-shaped scintillator. We report the detectors rise and decay times, the signal amplitude per unit of deposited energy, the energy resolution (FWHM) of the baseline after the optimum filter, at 5.9 keV X-ray of ^{55}Mn (LD), and at 2615 keV γ quanta of ^{208}Tl (LMO). We skip the computation of FWHM at 2615 keV for the 18 mK dataset due to poor statistics of the γ peak. Particle identification parameters (defined in Sec. 3.2) as light yield for $\gamma(\beta)$s $LY_{\gamma(\beta)}$ and a quenching factor for α particles QF_α, as well as the discrimination power between α and $\gamma(\beta)$ distributions $DP_{\alpha/\gamma(\beta)}$ for events selected in the 2.0–5.1 MeV energy range are also quoted.

Channel	Parameter	18 mK	12 mK
LD	Rise time (ms)	1.7	2.8
	Decay time (ms)	9.2	8.6
	Signal (μV/keV)	1.20	1.44
	FWHM (keV) at baseline	0.300(1)	0.210(1)
	FWHM (keV) at 5.9 keV X-ray	0.282(5)	0.315(4)
LMO	Rise time (ms)	18	25
	Decay time (ms)	150	160
	Signal (μV/keV)	0.017	0.036
	FWHM (keV) at baseline	4.2(2)	2.5(1)
	FWHM (keV) at 2615 keV γ	–	6.0(5)
LMO & LD	$LY_{\gamma(\beta)}$ (keV/MeV)	0.635(2)	0.638(1)
	QF_α (^{210}Po)	0.192(1)	0.199(4)
	$DP_{\alpha/\gamma(\beta)}$	7.4(4)	7.9(1)

written to disk for offline analysis. The Bessel-Thomson cut-off frequency was set at 300 Hz, as a compromise between the bandwidth of the LMO (slow) and LD (relatively fast).

We used around-3-week-long stable periods of data for the analysis at each regulated temperature, not affected by external events (e.g. power cuts). We select 314 h of physics data at each temperature and 65 and 220 h of the ^{232}Th calibration data at 18 and 12 mK, respectively.

The acquired data are triggered offline to tag discrete energy depositions. The triggered pulses are then processed by the optimum filter technique [**?**] to evaluate the signal amplitude (i.e. energy) and several pulse-shape parameters. In the reconstruction of the coincidences between the LMO and LD, we account for the LD faster response and correct for its constant time shift with respect to the LMO signal, similarly to the method described in [**?**].

3 Results

3.1 Detector performance

The performance parameters achieved by the LMO and LD in the 18 and 12 mK tests are listed in Table 1. The rise and decay time constants, defined respectively as time intervals of the (10–90)% rising edge and (90–30)% trailing edge relative to the signal maximum, of the LMO are ~0.02 and

~0.15 s, respectively. We expect the LD response to be faster by an order of magnitude because of the smaller heat capacity of both the Ge absorber and the NTD thermistor. The time constants obtained are in agreement with the results of previous investigations of similar size LMOs and LDs [**?** **?**]. It is worth noting that the time response of the bolometric detectors depend on the operation temperature and the sensor polarization (see, e.g., [**?**]). However, optimization of the detector time response[2] was out of the scope of the present study.

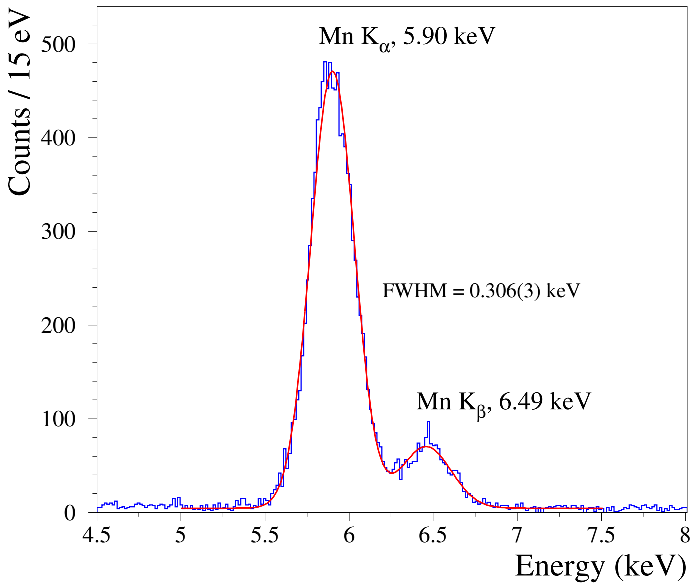

Figure 2. The energy spectrum of the ^{55}Fe X-ray source measured by a 1.4 g Ge bolometric light detector over 913 h (12 and 18 mK data) in the CROSS pulse tube based cryogenic facility at the Canfranc underground laboratory (Spain). A fit to the data by a model assuming a double-Gaussian function and a flat background component is shown by solid (red) line. The energy resolution (FWHM) is quoted for the 5.9 keV X-ray peak of Mn K$_\alpha$.

The LD signal amplitude per unit of deposited energy is 1.2 μV/keV at 18 mK and 1.4 μV/keV at 12 mK. The LMO signal amplitude is of course inferior, 17 nV/keV at 18 mK and doubles at 12 mK. Since the working points were not optimized to get the highest sensitivity, these results are good but not extraordinary among similar devices [**?** **?**].

The LD is calibrated with the 5.9 and 6.5 keV X-rays emitted by the ^{55}Fe source. The energy spectrum of the ^{55}Fe source gathered over 913 h of physics and thorium calibration runs is shown in Fig. 2. The almost fully resolved Mn K$_\alpha$/K$_\beta$ doublet is visible thanks to the high LD energy resolution: ≈0.3 keV FWHM at 5.9 keV. The baseline noise is 0.2–0.3 keV FWHM, demonstrating a reasonably low threshold. It is worth noting that such devices do not always show a high energy resolution even if characterized by ten(s) eV RMS noise[3], due to the position-dependent response

---

[2] In particular, to get the fastest response in view of the rejection of random coincidence events induced background in the ^{100}Mo $0\nu2\beta$ region of interest [**?** **?** **?**].

[3] For example, the Mn doublet resolution of 0.3–0.5 keV FWHM was measured with LDs made of 30–45 μm thick Ge wafers [**?**], while the 0.08 keV FWHM resolution was achieved by a 33 g Ge bolometer (⌀20×20 mm) characterized by a similar noise level [**?**].

of thin bolometers.

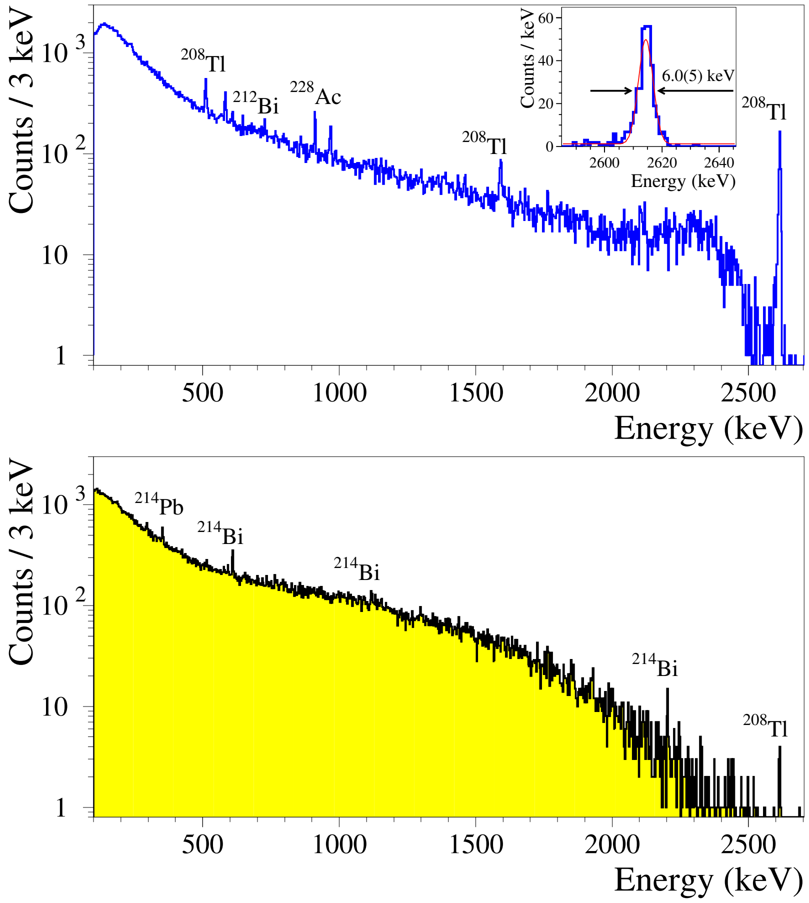

Figure 3. The energy spectra of $\gamma(\beta)$ events accumulated by the LMO over the calibration (285 h; top panel) and physics data (628 h; bottom panel) measurements in the C2U facility at the Canfranc underground laboratory. The most prominent γ peaks are labeled. The contribution of α events to the physics data has been removed with the scintillation light based particle identification (see text). The inset shows the γ peak with energy of 2615 keV in the calibration data together with a fit and the calculated energy resolution (FWHM).

We measured the LMO energy scale and resolution with the most intense gamma peaks in the thorium spectrum, illustrated in Fig. 3 (top panel). Because of the incomplete shielding, the physics data (Fig. 3, bottom panel) also exhibit several γ peaks from residual environmental radioactivity (daughters of ^{226}Ra and ^{228}Th sub-chains). The ^{238}U/^{234}U alpha source also emits β particles from ^{234m}Pa decays (Q_β = 2.27 MeV [?]), which, together with the ^{100}Mo $2\nu2\beta$ decays [?], are responsible for the most part of the continuum background above 0.5 MeV, seen in Fig. 3 (bottom panel).

The energy dependence of the LMO energy resolution is presented in Fig. 4. The results extracted from physics data are limited by the poor statistics. The detector demonstrates a good energy resolution in a wide energy interval exhibiting a peak width slightly increasing with energy, in agreement with early findings [? ?]. In particular, we achieved a 6 keV energy resolution (FWHM) for γ-ray quanta of ^{208}Tl with energy 2615 keV, and a 2.5 keV FWHM baseline noise.

The resolution at the $Q_{2\beta}$ of ^{100}Mo is expected to be very similar (Fig. 4). These results are in agreement with prior measurements for cylindrical LMOs [**?** **?** **?**], confirming an excellent bolometric performance independent of the crystal shape. It is also evident that a low baseline noise is crucial in obtaining a high energy resolution with a $Li_2{}^{100}MoO_4$ bolometer. It is worth noting, the lowest noise achieved with the LMO is a factor 2–4 worse than the best reported values for large-volume lithium molybdate bolometers [**?** **?**]. Thus, taking into account sub-optimal noise level of the present study, there is still room for improvement.

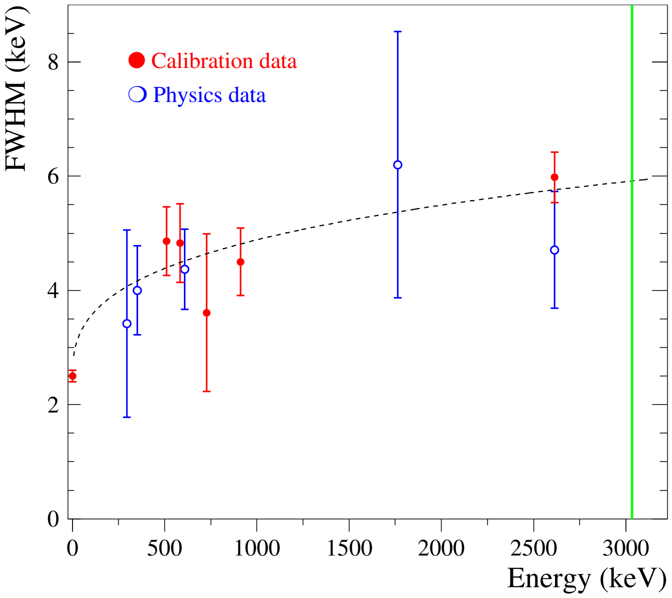

Figure 4. Energy dependence of the 279 g $Li_2{}^{100}MoO_4$ bolometer energy resolution (FWHM) measured in the calibration (filled circles; 12 mK) and physics (open circles; 18 and 12 mK) runs. The fitting curve is shown by the dashed line, while the solid line indicates the ^{100}Mo $Q_{2\beta}$.

3.2 Particle identification capability

Coincidences between the LMO and LD have been used to probe the scintillation based particle identification (PID). For each event triggered by the LMO we calculated a PID parameter, the so-called light yield (LY), defined as the ratio of the LD to LMO measured energy. The LY dependence on particle energy is shown in Fig. 5, where the population of $\gamma(\beta)$ events is clearly separated from α's. Such a powerful separation is achieved thanks to the quenching of the scintillation light for α particles with respect to $\gamma(\beta)$'s of the same energy and low noise of the LD. Different ionization properties lead also to a different amplitude measured by the LMO. Figure 5 shows a ~7% increase of an α event energy with respect to the gamma energy scale, in agreement with previous studies of LMO bolometers [**?** **?**]. This difference, called thermal quenching, hints at a possibility of PID by pulse-shape analysis of the heat channel itself [**?**], but it is by far less reproducible due to a strong dependence on the noise conditions[4].

---

[4] Since the present detector does not have the CROSS technology of the surface coating for PID purpose, we skip an analysis of pulse-shape discrimination of α events.

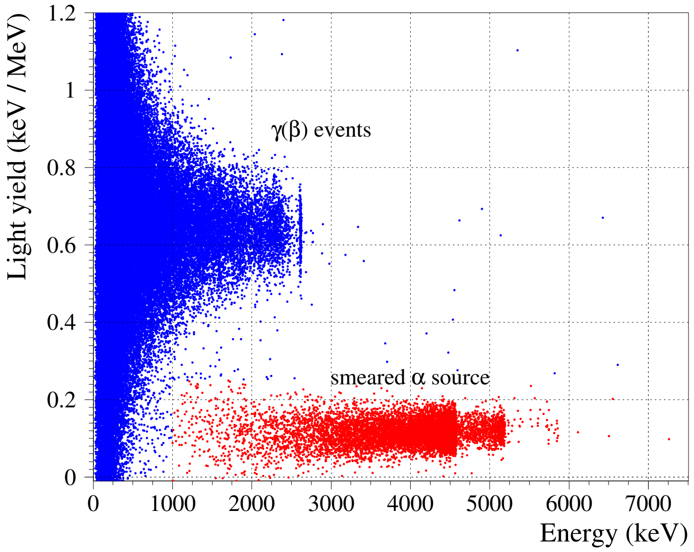

Figure 5. Light yield as a function of energy deposited in the LMO and measured in a 125 h long ^{232}Th calibration at 12 mK. The energy scale is calibrated with γ quanta. The population of $\gamma(\beta)$ events is clearly separated from the α events, mainly originated by the ^{238}U/^{234}U smeared α source. The α events shown in red were selected above 1 MeV with a LY cut below 0.25 keV/MeV.

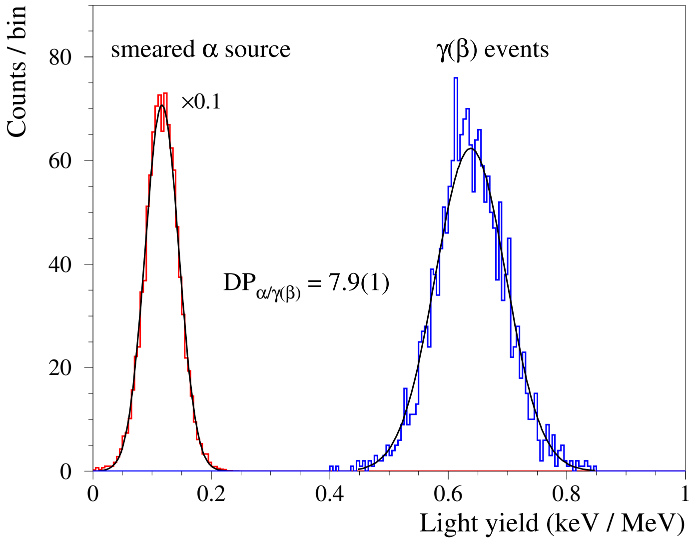

Figure 6. The light yield distributions for α and $\gamma(\beta)$ particles, selected in the 2.0–5.1 MeV energy interval. The former distribution is rescaled by a factor 0.1 to improve the visibility of the later one. A Gaussian fit to each distribution is shown by a solid line. The discrimination power between the two populations is ~8.

In order to investigate a LY-based $\alpha/\gamma(\beta)$ separation close to the ^{100}Mo $0\nu2\beta$ region of interest (ROI), we selected events within the 2.0–5.1 MeV energy range and a LY interval of 0.4–1.0 keV/MeV for $\gamma(\beta)$'s and 0–0.25 keV/MeV for α's; both are shown in Fig. 6. A Gaussian fit to each distribution provides a LY mean value (μ) and standard deviation (σ), which we used to calculate the so-called discrimination power defined as

$$DP_{\alpha/\gamma(\beta)} = \left|\mu_{\gamma(\beta)} - \mu_{\alpha}\right| / \sqrt{\sigma^2_{\gamma(\beta)} + \sigma^2_{\alpha}}. \tag{3.1}$$

The $DP_{\alpha/\gamma(\beta)}$ based on the present data is around 8 (Table 1), meaning about $8\sigma_{\alpha}$ of alpha event rejection while keeping almost 100% of $\gamma(\beta)$'s. This rejection power fully satisfies the CUPID goal of identifying 99.9% of alpha particles (corresponding to $DP_{\alpha/\gamma(\beta)} \sim 3.1$).

The LMO light yield for $\gamma(\beta)$ events ($LY_{\gamma(\beta)}$) was found to be 0.64 keV/MeV, similar to one measured with cylindrical shaped LMOs of ⌀44×45 mm size [**?** **?** **?**]. However, in the present study the light collection efficiency was affected by the smaller area of the LD (15 cm^2) with respect to the LMO surface facing it (20 cm^2) and by the entrance window of the Cu holder (⌀45 mm). Thus, considering only the direct light, the $LY_{\gamma(\beta)}$ is expected to be ∼ 0.85 keV/MeV, once a 45 mm side square LD is coupled to the LMO. In case of the use of two LDs, the LY should be roughly doubled, as demonstrated by CUPID-Mo [**?** **?**]. The quenching factor (QF_{α}) for α particles of ^{210}Po observed in the data (see the next section) is 0.2 [5], in agreement with the previous data [**?** **?** **?**].

3.3 Li$_2$^{100}MoO$_4$ crystal radiopurity

A highly-efficient PID together with a good energy resolution of the LMO operated over four weeks of background measurements allow us to quantify the Li$_2$^{100}MoO$_4$ radiopurity with a high sensitivity. The spectrum of alpha events selected from the physics data (and recalibrated to α energy) is presented in Fig. 7; the energy interval covers most Q_{α}-values of radionuclides from the U/Th chains. As it is seen in Fig. 7, the use of the ^{238}U/^{234}U smeared α source prevents estimation of the alpha activity of ^{232}Th, ^{238}U and some of the daughters with $Q_{\alpha} \leq 4.8$ MeV. However, we can investigate a possible contamination by ^{226}Ra and ^{228}Th, which are the most harmful contaminants for $0\nu2\beta$ searches.

The energy region above 4.8 MeV contains only two peak-like structures both ascribed to ^{210}Po α events, and originated by the ^{210}Pb contamination [**?**]. A clear peak at 5.4 MeV is induced by the ^{210}Po decays in the Li$_2$^{100}MoO$_4$ crystal bulk with the activity of 80(12) μBq/kg. A ^{210}Po (^{210}Pb) bulk contamination on the level of ten(s)–hundred(s) μBq/kg is typical for Li$_2$^{100}MoO$_4$ crystals [**?** **?** **?** **?**]. A broad distribution peaked at 5.3 MeV is caused by the ^{210}Po decay on the surface of materials facing the LMO (a 0.1 MeV energy is taken away by the ^{206}Pb nuclear recoil). The decays of ^{210}Po at surfaces of the detector materials can populate the ^{100}Mo $0\nu2\beta$ ROI as energy-degraded alpha events, but they can be easily rejected thanks to the efficient PID of Li$_2$^{100}MoO$_4$ scintillating bolometers. Also, the total rate of ^{210}Po events (∼0.06 mHz) is rather low to be a notable source of pile-ups, which are of certain concern for slow response thermal detectors [**?**].

---

[5] Such a parameter is typically quoted without the correction from the thermal quenching and we follow that convention here.

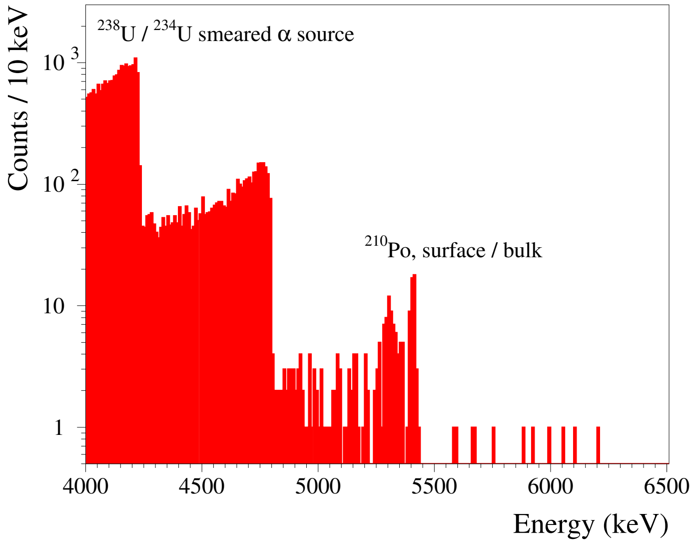

Figure 7. A part of the α energy spectrum accumulated by the LMO operated over 628 h in the CROSS underground cryostat in Canfranc. The energy interval covers the Q_α-values of the most α-active radionuclides from U/Th decay chains. In addition to a dominant contribution from the used ^{238}U/^{234}U source, the spectrum exhibits only two populations of ^{210}Po originated by external (surface of nearby materials) or internal (crystal bulk) contaminations of the detector.

The spectrum shows no other structures, so we can only set limits on other radionuclide contaminations. In order to be conservative, we considered all events within 25 keV of each expected peak location. The background (1 count per 50 keV) was estimated in the 5.65–5.75 and 5.85–5.95 MeV energy intervals, containing no Q_α-value of U/Th radionuclides. The data exhibit no events of ^{228}Th (Q_α = 5520 keV [**?**]) and two counts of ^{222}Rn (Q_α = 5590 keV [**?**]; a daughter of ^{226}Ra), thus we place 90 confidence level (C.L.) upper limits of 1.6 and 4.9 counts, respectively [**?**]. A selection efficiency of 95.7% was estimated using alpha events of the ^{238}U/^{234}U smeared α source, distributed in the 3.5–4.8 MeV energy interval. Therefore, the activity of ^{228}Th and ^{226}Ra in the Li$_2$^{100}MoO$_4$ crystal bulk is below 3 and 8 μBq/kg at 90% C.L., respectively. Taking into account the reasonably short half-lives of ^{228}Ra (5.75 yr [**?**]) and ^{228}Th (1.91 yr [**?**]), the limit on the ^{228}Th activity can also represent the ^{232}Th contamination in the crystals, as e.g. seen in [**? ? ?**].

The limits on the ^{228}Th and ^{226}Ra activity in the studied Li$_2$^{100}MoO$_4$ crystal are on the same level as reported by LUMINEU [**? ?**], which were obtained by the analysis of a comparable exposure. A significantly larger exposure of the CUPID-Mo experiment [**? ? ?**] shows that the level of remaining contaminants in Li$_2$^{100}MoO$_4$ scintillators can be even an order of magnitude lower. As the protocol of the CROSS crystal production was the one adopted by LUMINEU and CUPID-Mo, it seems natural to assume the radiopurity of the CROSS crystals to be similar to that of CUPID-Mo ones. It is worth noting that the ^{228}Th (^{232}Th) and ^{226}Ra contamination on the level of 10 μBq/kg is compatible with a background contribution below 10^{-4} counts/yr/kg/keV to the ^{100}Mo $0\nu2\beta$ ROI, and it is fully acceptable not only for the medium-scale CROSS experiment (with ~10 kg detector mass), but also for the tonne-scale extension of CUPID.

4 Conclusions

We report that performance and radiopurity of a scintillating bolometer based on a large cubic-shaped $Li_2{}^{100}MoO_4$ crystal —randomly taken from 32 identical crystals (with a 45 mm side and a mass of 0.28 kg each) of the CROSS $0\nu2\beta$ project— are similar to those of cylindrical 0.2 kg $Li_2{}^{100}MoO_4$ bolometers, used in LUMINEU and CUPID-Mo 2β experiments. In particular, the $Li_2{}^{100}MoO_4$ detector energy resolution at 2615 keV γ quanta (as well as its approximation to 3034 keV, the ^{100}Mo 2β decay energy) is 6 keV FWHM. A scintillation light yield of the cubic-shaped crystal, 0.64 keV/MeV for $\gamma(\beta)$'s, is compatible to that of cylindrical crystals. However, the measured light yield is affected by about 30% lower detection surface of the optical bolometer with respect to the nearby $Li_2{}^{100}MoO_4$ crystal face. In spite of sub-optimal light collection, a full separation ($\sim 8\sigma$) between α and $\gamma(\beta)$ events above 2 MeV has been achieved. A high radiopurity of the cubic-shaped $Li_2{}^{100}MoO_4$ crystal was also demonstrated by the present study, where only ^{210}Po is detected with the activity of 80(12) μBq/kg, while the content of ^{228}Th and ^{226}Ra (the most harmful radionuclides from U/Th families for $0\nu2\beta$ searches) is estimated to be less than 3 and 8 μBq/kg, respectively.

The performed investigation additionally proves the excellent prospects of $Li_2{}^{100}MoO_4$ scintillating bolometers for high-sensitivity $0\nu2\beta$ decay searches. The cubic shape of large-volume ($\sim$90 cm^3) $Li_2{}^{100}MoO_4$ crystals allows a more compact detector array structure and thus the deployment of a larger isotope mass in the experimental volume, as well as an increased efficiency of multi-site event detection. In view of these results, large-mass ($\sim$0.3 kg) radiopure cubic-shaped $Li_2{}^{100}MoO_4$ crystals operated as bolometers satisfy the demands of the CROSS and CUPID projects.

Acknowledgments

The CROSS and CUPID Collaborations thank the directors and staff of the Laboratorio Subterráneo de Canfranc and the technical staff of our laboratories. This work was supported by the Istituto Nazionale di Fisica Nucleare (INFN); by the European Research Council (ERC) under the European Union Horizon 2020 program (H2020/2014-2020) with the ERC Advanced Grant no. 742345 (ERC-2016-ADG, project CROSS) and the Marie Sklodowska-Curie Grant Agreement No. 754496; by the Italian Ministry of University and Research (MIUR) through the grant Progetti di ricerca di Rilevante Interesse Nazionale (PRIN 2017, grant no. 2017FJZMCJ); by the US National Science Foundation under Grant Nos. NSF-PHY-1614611 and NSF-PHY-1401832; by the P2IO LabEx (ANR-10-LABX-0038) managed by the Agence Nationale de la Recherche (France). This material is also based upon work supported by the US Department of Energy (DOE) Office of Science under Contract Nos. DE-AC02-05CH11231 and DE-AC02-06CH11357; and by the DOE Office of Science, Office of Nuclear Physics under Contract Nos. DE-FG02-08ER41551, DE-SC0011091, DE-SC0012654, DE-SC0019316, DE-SC0019368, and DE-SC0020423. This work was also supported by the Russian Science Foundation under grant No. 18-12-00003 and the National Research Foundation of Ukraine under Grant No. 2020.02/0011.